Journal of Inflammation Research

Dovepress
open access to scientific and medical research

Open Access Full Text Article

ORIGINAL RESEARCH

Sinomenine Ameliorates IL-1β-Induced Intervertebral Disc Degeneration in Rats Through Suppressing Inflammation and Oxidative Stress via Keap1/Nrf2/NF-κB Signaling Pathways

Gongbiao Lu[1,2,*], Cunxin Zhang[2,*], Kang Li[2], Kai Gao[3], Maoqing Fu[2], Chaoliang Lyu[2], Zhengxue Quan[1]

[1]Department of Spine Surgery, the First Affiliated Hospital of Chongqing Medical University, Chongqing, 400042, People's Republic of China; [2]Department of Spine Surgery, Jining No.1 People's Hospital, Jining, 272011, People's Republic of China; [3]Department of Orthopaedics, Jining No.1 People's Hospital, Jining, 272011, People's Republic of China

*These authors contributed equally to this work

Correspondence: Zhengxue Quan, Department of Spine Surgery, the First Affiliated Hospital of Chongqing Medical University, No. 1 Youyi Road, Yuzhong District, Chongqing, 400042, People's Republic of China, Tel +86 13608321800, Fax +86-023-68811360, Email Quanzx18@126.com; Chaoliang Lyu, Department of Spine Surgery, Jining No.1 People's Hospital, No. 6 Healthy Road, Rencheng District, Jining, 272011, People's Republic of China, Tel +86 15265775628, Fax +86-0537- 2253252, Email lvchaolianggk@163.com

Purpose: To investigate the molecular mechanism underlying the inhibitory effect of sinomenine (SN) on interleukin-1β (IL-1β)-induced apoptosis in nucleus pulposus cells (NPCs), and to evaluate the potential role of SN in preventing intervertebral disk degeneration (IDD).

Methods: The Rat NPCs were cultured in vitro and identified using Hematoxylin-Eosin (HE) staining, toluidine blue staining, and immunofluorescence analysis. NPCs were pretreated with or without SN, then induced with IL-1β to assess cell viability, ROS levels, apoptotic rates, and wound healing ability. Relevant protein expression was detected using Elisa, qPCR and Western Blot techniques. NPCs were pretreated with SN, either alone or in combination with Nrf2-IN-1 or SC, before being induced to undergo apoptosis by IL-1β. Apoptosis was detected using Hoechst staining, while qPCR and Western Blot techniques assessed protein expression. Rat caudal intervertebral discs were induced with IDD, with or without SN injection, and then co-injected with IL-1β. The levels of IDD were evaluated using HE staining and modified saffron-O-fix green cartilage staining. Relevant protein expression was detected using Elisa, qPCR, and Western Blot techniques.

Results: IL-1β significantly reduced NPC activity, induced ROS accumulation and apoptosis, decreased cell healing rate, promoted the expression and secretion of inflammatory factors, and inhibited extracellular matrix synthesis. However, pretreatment with SN effectively reversed these effects. Inhibition of the Keap1/Nrf2 signaling pathway or activation of the NF-κB signaling pathway significantly attenuated the cytoprotective effects of SN and increased apoptosis. Acupuncture combined with IL-1β injection markedly induced intervertebral disc degeneration in rat caudal spine, upregulated inflammatory factors expression and secretion, and downregulated extracellular matrix synthesis. SN intervention notably enhanced antioxidant enzyme expression and reversed these outcomes.

Conclusion: SN can prevent IL-1β-induced apoptosis of NPCs and ameliorate IDD by activating the Keap1/Nrf2 pathway and inhibiting the NF-κB signaling pathway.

Keywords: sinomenine, intervertebral disc degeneration, nucleus pulposus cells, apoptosis, Nrf2, NF-κB

Introduction

In 1932, Barr initially proposed that lumbar disc herniation (LDH) could be the etiology of low back pain (LBP) and radiating pain in lower extremities, and introduced the concept and treatment of LDH.[1,2] Current studies suggest that the

Received: 25 August 2023
Accepted: 17 October 2023
Published: 20 October 2023

main factors of LPB and lower limb radialpain induced by LDH are not only mechanical compression of nerve roots by Nucleus Pulposus Tissue (NPT), but also the stimulation of local inflammatory factors. Lu et al found that infiltration and activation of macrophages and microglia significantly increased the release of colony-stimulating factor 5622 during LDH-induced sciatica in mice. Treatment with PLX1, a specific antagonist for colony-stimulating factor 5622 receptor, effectively relieved LDH-induced sciatica. Kitti et al have demonstrated the significant involvement of pro-inflammatory cytokines, including TNF-α, IL-6, and IL-8, as well as anti-inflammatory cytokines such as IL-4 and IL-10 in the inflammatory response induced by LDH. Clinical studies have shown promising results with the use of TNF-α inhibitors and IL-6 inhibitors for treating low back pain and sciatica.[3] The currently acknowledged initiating factors of intervertebral disc degeneration (IDD) encompass oxidative stress, aging, nutritional deficiencies, genetic susceptibility and mechanical overload.[4] However, Wang et al have discovered that early degenerative intervertebral discs (IVDs) contain a significant amount of inflammatory factors, primarily including IL-1β, TNF, and IL-18.[5] These inflammatory factors, which activate NLRP3 inflammasomes and induce cellular damage, result in reduced quantity and quality of nucleus pulposus cells (NPCs), ultimately leading to IDD.[6,7] Therefore, it is crucial to inhibit the inflammatory response within the IVD and reduce the apoptosis of NPCs in order to prevent IDD and LDH.

Sinomenine (SN) is an alkaloid extracted from the dried vine stems of sinomenium acutum. It possesses analgesic,[8] anti-inflammatory[9] and antioxidant[10] properties. Liu et al demonstrated that SN exerts an inhibitory effect on the progression of rheumatoid arthritis by modulating the secretion of inflammatory cytokines and regulating mononuclear/macrophage subsets.[11] Fan et al discovered that SN can protect PC12 neuronal cells from hydrogen peroxide-induced cytotoxicity and oxidative stress by upregulating the endogenous antioxidant system in a reactive oxygen-dependent manner.[10] Meanwhile, zeng et al found that SN could inhibit LPS-induced macrophage immune responses through blocking the activated TLR4/NF-κB signaling pathway.[12] In summary, the principal mechanisms through which SN exerts its effects are anti-inflammatory and antioxidant in nature. Consequently, we postulate that SN may also confer anti-inflammatory and antioxidant benefits upon NPCs, thereby impeding inflammatory factor-mediated apoptosis of these cells and ultimately thwarting IDD.

Whether SN can inhibit IDD by suppressing oxidative stress and inflammatory responses has not been previously reported. In this study, we have innovatively linked the inhibition of oxidative stress and inflammatory response by SN with apoptosis of NPCs. The aim was to investigate the role and mechanism of SN in IL-1β-induced apoptosis of NPCs and IDD, providing new directions and theories for the prevention and treatment of IDD.

Materials and Methods

Ethics Statement

All the animal procedures were performed in accordance with the Guidelines for Care and Use of Laboratory Animals of the National Institutes of Health. All animal experiments were approved by the Institutional Review Board (or Ethics Committee) of Jining No.1 People's Hospital (JNRM-2022-DW-060).

Cell Culture

After aseptically obtaining the NPT from four eight-week-old SD rats, the cells were enzymatically dissociated using 0.25% trypsin (Upsilon, Beijing, China) at 37°C for 20 minutes followed by digestion with 0.2% type II collagenase (Solarbio, Beijing, China) at 37°C for one hour. The supernatant was discarded after centrifugation and the cells were resuspended in fresh cell culture medium. The cell density was adjusted to 1.0×10^6/mL before being seeded into cell culture flasks and placed in an incubator.

Cell Identification

HE staining was employed to visualize the morphology of NPCs, while toluidine blue staining was utilized to examine the distribution of aggregated proteoglycans. Immunofluorescence staining was applied to observe the expression of type II collagen and aggregated proteoglycans. For immunofluorescence staining, NPCs were fixed with 4% paraformaldehyde solution (Solarbio, Beijing, China) for 30min and then infiltrated with 0.5% Triton X-100 solution (Solarbio, Beijing, China) for 30min. After incubation with 5% blocking goat serum solution (Solarbio, Beijing, China) for 30min at room temperature, collagen type II

(Affinity Biosciences, Nanjing, China) and aggrecan (Affinity Biosciences, China, Affinity Biosciences, Nanjing, China) were closed overnight at 4 ° C. The fluorescent secondary antibody (EARTHOX, San Francisco, CA, USA) was then incubated for 1h at 37 ° C in the dark. After further incubation with DAPI staining solution (Beyotime, Nanjing, China) at room temperature in the dark for 5min, the plates were washed 5 times with PBS, sealed, and observed under an inverted fluorescence microscope (Olympus, Japan) and photographed.

Cell Viability Assay

Following the protocol of the CCK-8 kit (Dojindo, Japan), the original culture medium was discarded after treatment with NPCs. Subsequently, 100μL of FBS-free culture medium and 10μL of CCK-8 solution were added to each well (6 wells per group). The microplates were then incubated at 37°C in a dark environment for 1–4 hours before measuring absorbance at 450nm using a multifunctional microplate reader (Bio Tek Instruments, USA).

Measurement of ROS

According to the protocol of a reactive oxygen species detection kit (Beyotime, Nanjing, China), following NPCs treatment, the original culture medium was discarded and 100μL of 10μM 2',7'-dichlorofluorescin diacetate (DCFH-DA) solution was added to each well (6 wells per group). In the positive control group, ROSup was added and incubated at 37°C in darkness for 20 minutes. After washing off excess staining solution with PBS, fluorescence intensity was measured using a multifunctional microplate reader (BioTek Instruments, USA).

Cell Scratch Assay

A 10μL pipette tip was utilized to create a straight scratch in the center of the Petri dish. Following PBS washing, the width of the scratch was documented, marked, and measured using an inverted microscope (Olympus, Japan). The width of each scratch was measured at six different locations. After 24 hours, the same position was re-photographed and measured for scratch width.

Flow Cytometry Analysis

According to the protocol of Annexin V-FITC/PI Apoptosis Detection kit (Vazyme Biotech, Nanjing, China), NPCs from each group were harvested by digestion and resuspended in 100μL loading buffer. In the experimental group, 5μL Annexin V-FITC staining solution and PI staining solution were added simultaneously (3 petri dishes per group). The Annexin V-FITC group was treated with 5μL of Annexin V-FITC staining solution while the PI group received 5μL of PI staining solution. The untreated double negative group was incubated at room temperature in the dark for 10 minutes, followed by resuspension with 400μL Loading Buffer. The apoptosis rate was then determined using flow cytometry (Beckman, USA).

Hoechst Staining

NPCs were fixed for 10 minutes, washed twice with PBS, and then stained with Hoechst staining solution for 5 minutes according to the instructions of the Hoechst staining kit (Beyotime, Nanjing, China). The slides were subsequently sealed and observed under an inverted fluorescence microscope (Olympus, Japan), followed by photography. It was an independent observational experiment.

Identification of Inflammatory Biomarkers Within NPCs and IVD

According to the instructions of Rat Tumor necrosis Factor α (TNF-α) ELISA KIT (SPbio, Wuhan, China), Rat Interleukin 1β (IL-1β) ELISA Kit (SPbio, Wuhan, China), Rat Interleukin 6 (IL- 6) ELISA KIT (SPbio, Wuhan, China), Rat Interleukin 17 (IL-17) ELISA Kit (SPbio, Wuhan, China) instructions for the detection of TNF-α, IL-1β, IL-6 and IL-17 in NPCs and IVD, and three replicates were set for each group.

RNA Extraction and Quantitative Reverse Transcription PCR (qRT-PCR)

Total RNA was extracted from NPCs/NPT using the Fast Pure Cell/Tissue Total RNA Isolation Kit V2 (Vazyme Biotech, Nanjing, China) following the manufacturer's instructions. Reverse transcription into cDNA was performed with HiScript

III RT SuperMix for qPCR (+gDNA wiper) (Vazyme Biotech, Nanjing, China) according to the recommended protocol. According to the protocol of Taq Pro Universal SYBR qPCR Master Mix (Vazyme Biotech, Nanjing, China), qPCR reactions were conducted on a Bio-Rad CFX Maestro 2.2 Real-Time PCR System (Bio-Rad, Hercules, CA, USA) with β-actin serving as an internal control. Three replicates were set up for each group. The primers utilized in this study were purchased from Sangon Biotech (Shanghai) Co., Ltd.(China). The primer sequences are presented in Table 1.

Table 1 Sequences of Primers Used in the Study

Gene	Direction	Sequences
MMP-3	Forward(5'-3')	TTGATGGGCCTGGAATGGTC
	Reverse(5'-3')	CAGGGAGTGGCCAAGTTCAT
MMP-13	Forward(5'-3')	ACCATCCTGTGACTCTTGCG
	Reverse(5'-3')	TTCACCCACATCAGGCACTC
Decorin	Forward(5'-3')	AGAGATCAAAGAGGGGGCCT
	Reverse(5'-3')	TTGGGCAATTTTTCGGGCAG
COL2A1	Forward(5'-3')	TCCTACAATGTCAGGGCCAG
	Reverse(5'-3')	TCATCGCAGAGGACATTCCC
TNF-α	Forward(5'-3')	AGGCACTCCCCCAAAAGATG
	Reverse(5'-3')	CCACTTGGTGGTTTGTGAGTG
IL-1β	Forward(5'-3')	GCCACCTTTTGACAGTGATG
	Reverse(5'-3')	GTGCTGCTGCGAGATTTGAA
IL-6	Forward(5'-3')	CTCTCCGCAAGAGACTTCCA
	Reverse(5'-3')	CTCCTCTCCGGACTTGTGAA
IL-17	Forward(5'-3')	GGGAAGTTGGACCACCACAT
	Reverse(5'-3')	GCATGGCGGACAATAGAGGA
Keap1	Forward(5'-3')	GATGAACGGGGCAGTCATGT
	Reverse(5'-3')	AAGAACTCCTCCTCCCCGAA
Nrf2	Forward(5'-3')	CAGAGTGATGGTTGCCCACT
	Reverse(5'-3')	CACACACTTTCTGCGTGCTC
HO-1	Forward(5'-3')	ACAGAAGAGGCTAAGACCGC
	Reverse(5'-3')	TAAGGAGAGCAGAAGCCAAGAG
NQO-1	Forward(5'-3')	ATTGTATTGGCCCACGCAGA
	Reverse(5'-3')	GATTCGACCACCTCCCATCC
NF-κB	Forward(5'-3')	CTGGAGCAAGCCATTAGCCA
	Reverse(5'-3')	CAGATCTTGAGCTCGGCAGT
β-actin	Forward(5'-3')	ATCGCTGCGCTGGTCG
	Reverse(5'-3')	GTCCTTCTGACCCATTCCCA

Western Blot

Cells or tissues were lysed in a homogenizer (Jingxin, China) for 45 seconds at 60 Hz after being added to a mixture of RIPA lysate (Beyotime, Nanjing, China), phenylmethylsulfonyl fluoride (PMSF) (Beyotime, Nanjing, China), and protease phosphatase inhibitor mixture (Beyotime, Nanjing, China) in a ratio of 100:1:2. The supernatant was subjected to centrifugation at 14000g for 15 minutes at 4°C, and the sample concentration was determined using the BCA Protein Quantification Kit (Vazyme Biotech, Nanjing, China). The remaining sample was supplemented with a volume of 5×SDS-PAGE protein loading buffer (Beyotime, Nanjing, China) equal to one-fourth of its own volume and heated in a water bath at 100°C for 5–6 minutes. Protein samples were separated by electrophoresis on SDS-PAGE gels (Beyotime, Nanjing, China) and subsequently transferred onto membranes. The primary antibodies were incubated overnight at 4°C, followed by incubation with secondary antibodies at room temperature for 1 hour. PVDF membranes were treated with ECL working solution (Vazyme Biotech, Nanjing, China) and visualized using a fully automated chemiluminescence image analysis system (Tanon, Shanghai, China). The grayscale values of each target protein were quantified using Image J software. Each experiment was repeated three times. Decorin (DCN) antibody, alpha 1 type II collagen (COL2A1) antibody, nuclear factor erythroid 2-related factor 2 (Nrf2) antibody, phosphorylated Nrf2 antibody, Keap1 antibody, matrix metalloproteinase 3 (MMP3) antibody, matrix metalloproteinase 13 (MMP13) antibody, nuclear factor kappa-light-chain-enhancer of activated B cells (NF-κB) antibody and phosphorylated NF-κB antibody were procured from Affinity Biosciences (China), while heme oxygenase 1 (HO-1) antibody and NAD(P)H quinone dehydrogenase 1 (NQO-1) antibody were obtained from Abcam (Cambridge, UK).

IDD Model

18 eight-week-old Sprague-Dawley rats were randomly allocated into three groups: control, model and treatment group, with six rats in each group. In the model group, 5μL of recombinant rat IL-1β protein (ABclonal, China) at a concentration of 20μg/mL was injected into the annulus fibrosus using a 24G syringe needle. The treatment group received an additional injection of 5μL SN (MedChemExpress, New Jersey, USA) at a concentration of 4μM compared to the model group. IVD degeneration was observed after one month.

Safranine O-Fast Green FCF Cartilage Stain

According to the protocol of Modified Safranine O-Fast Green FCF Cartilage Stain Kit (Solarbio, China), IVD paraffin sections were dewaxed, rinsed in water, immersed in freshly prepared Weigert's iron hematoxylin solution for 5 minutes and then washed in water. The sections were swiftly rinsed with a dilute acid solution for 10 seconds, followed by a distilled water rinse for 10 minutes. The residual solid green stain was removed and the sections were subsequently dehydrated, made transparent, and sealed with neutral resin before being scanned using a digital section scanner (Jiangfeng Bio, China).

Statistical Analysis

All experimental results were analyzed using SPSS statistical software (IBM Corporation, USA, version 27.0) for data analysis and GraphPad Prism software (GraphPad Software, USA, version 6.0) was utilized for statistical plotting. The distribution of the data was assessed by means of the Shapiro–Wilk test in conjunction with a normal Q-Q plot. For quantitative data, one-way analysis of variance (ANOVA) was conducted followed by post hoc tests using either the Bonferroni or Tamhane's method. The results were presented as mean ± standard deviation and statistical significance was determined at $P<0.05$ level.

Results

Morphological Examination of NPCs

NPCs exhibited various morphologies, including short rod-shaped, triangular, polygonal, and short spindle-shaped forms as observed under optical inverted microscopy (Figure 1A). HE staining revealed blue-colored nuclei and pink cytoplasm in NPCs. Most cells were single-nucleated while a few dividing cells displayed double nucleation (Figure 1B). Toluidine blue staining revealed that the nuclei of NPCs exhibited a deep blue hue, while the cytoplasm contained aggregated proteoglycans that were also acidic and stained blue. The intensity of the blue coloring increased as it approached the nucleus (Figure 1C). Immunofluorescence staining demonstrated that Collagen II in NPCs emitted red fluorescence, whereas Aggrecan displayed green fluorescence. The

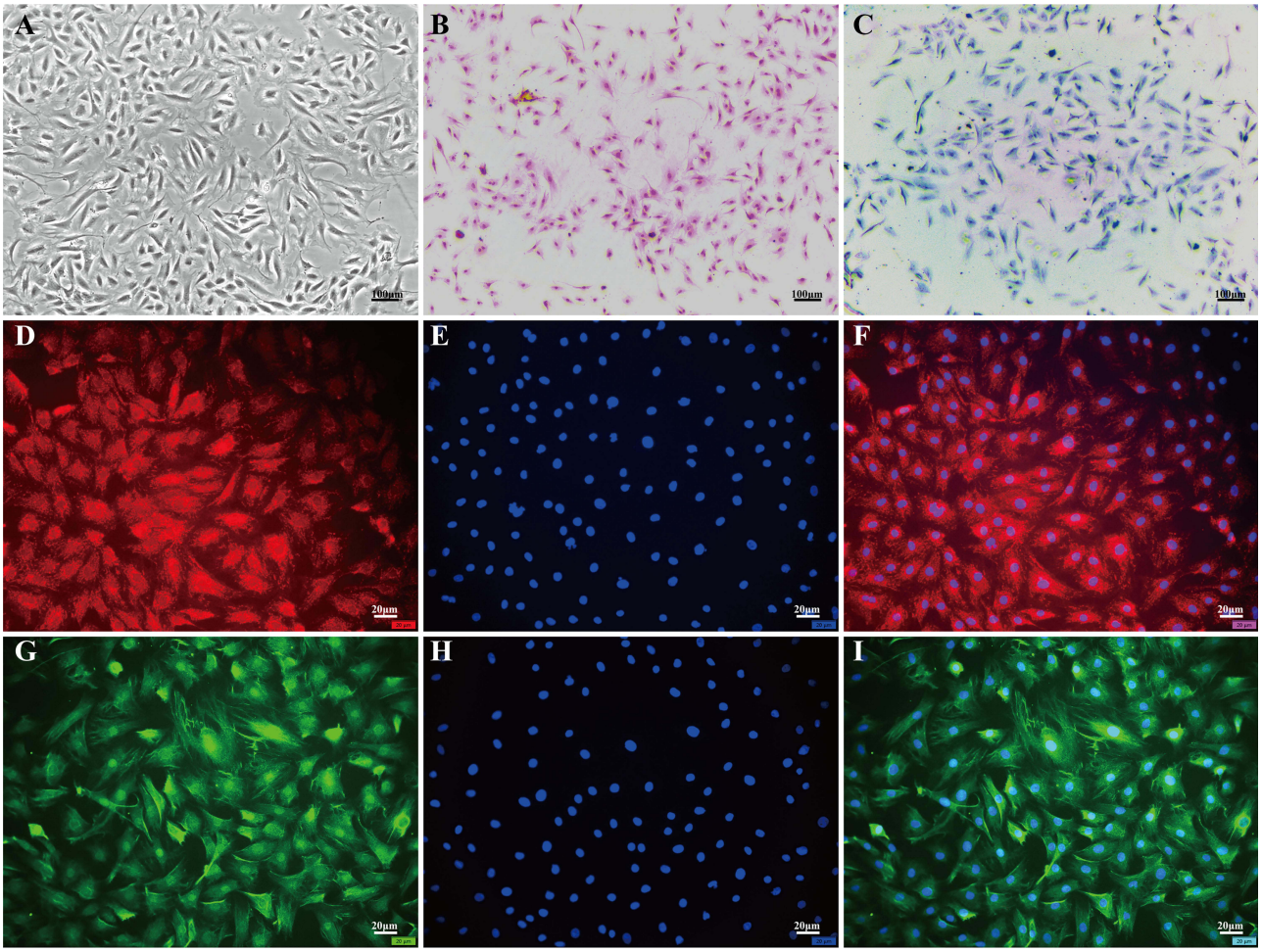

Figure 1 Morphological examination of NPCs. (**A**) Morphology of nucleus pulposus cells (NPCs) observed under an optical inverted microscope. (**B**) Hematoxylin and eosin staining revealed blue nuclei and pink cytoplasm in NPCs. (**C**) Toluidine blue staining showed dark blue nuclei and light blue cytoplasm in NPCs. (**D-F**) Collagen II immunofluorescence staining exhibited red fluorescence in NPCs. (**G-I**) Aggrecan immunofluorescence staining displayed green fluorescence in NPCs. The scale for (**A-C**) is 100μm, while the scale for (**D-I**) is 20μm.
Abbreviation: NPCs: Nucleus Pulposus Cells.

closer to the nucleus, the stronger was the fluorescence intensity observed; meanwhile, the nucleus itself showed blue fluorescence (Figure 1D-I).

SN Inhibits IL-1β-Induced Cytotoxicity in NPCs

SN is an alkaloid that consists of a pyrrole ring and an indole ring, with the molecular formula C22H26N2O2 and a molecular weight of 350.46 g/mol (Figure 2A). Cytotoxicity assays revealed that the safe concentration range of SN was 0–4 μM. The proliferative activity of NPCs decreased significantly with increasing concentrations above 4 μM, thus we determined 4 μM as the optimal drug concentration[13] (Figure 2B). To replicate the inflammatory microenvironment of IDD in vitro, we induced NPCs inflammation using IL-1β to simulate the pathological state of IDD. The results indicated that treatment with IL-1β for 24 hours led to a significant reduction in the cellular activity and wound healing capacity of NPCs, accompanied by a marked increase in ROS content and apoptosis. However, pretreatment with SN for 8 hours resulted in a substantial improvement in cell activity and wound healing capacity, along with a notable decrease in ROS content and apoptosis (Figure 2C-O).

SN Inhibited IL-1β-Induced Inflammation and Improved Cell Phenotype in NPCs

The qPCR and ELisa results demonstrated a significant increase in the expression of IL-1β, IL-6, IL-17, and TNF-α in NPCs after 24 hours of treatment with IL-1β. Furthermore, even after 8 hours of SN pretreatment, the inflammatory factor expression remained significantly higher than that observed in the control group but was significantly lower than

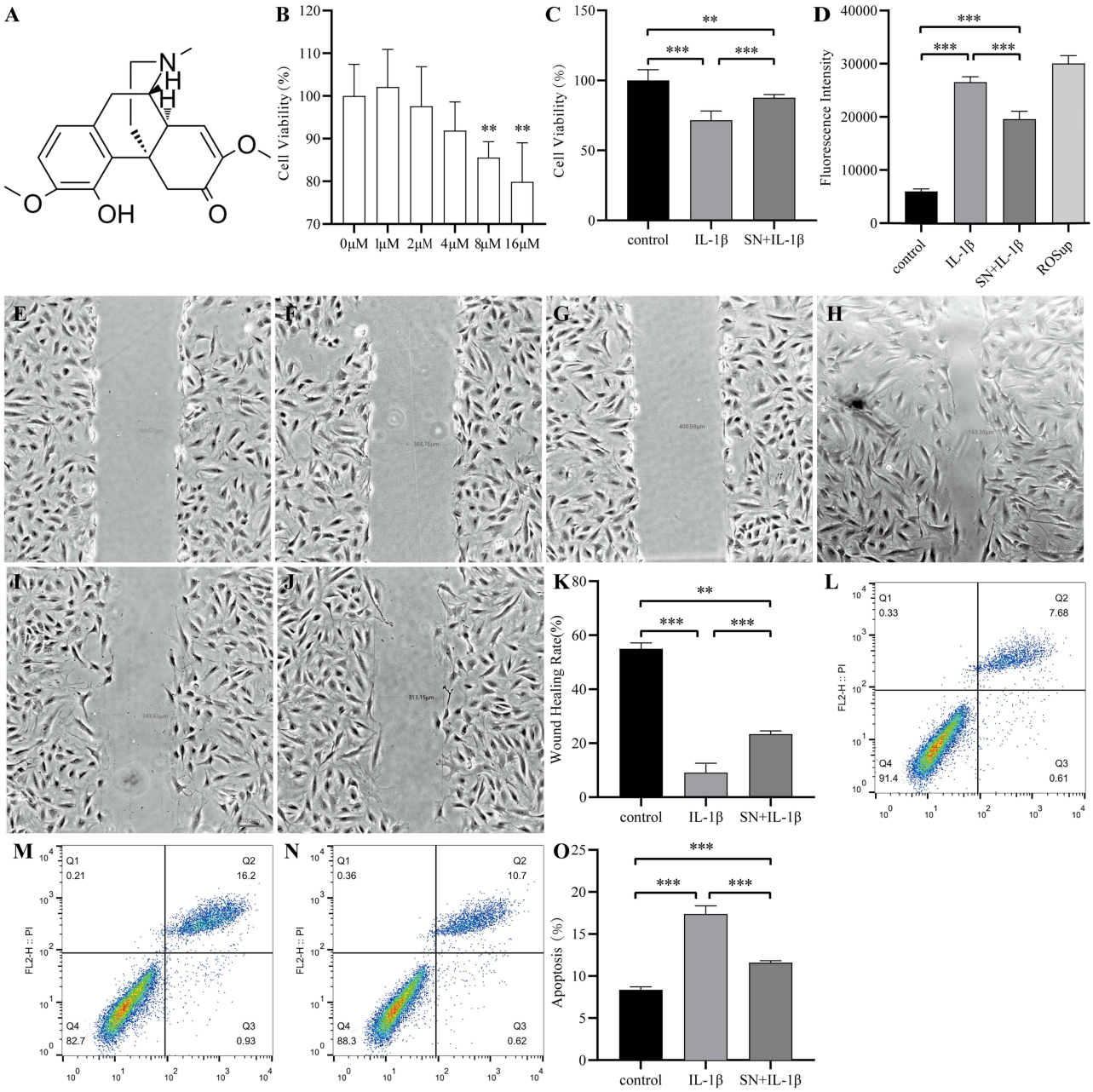

Figure 2 SN inhibits IL-1β-induced cytotoxicity of NPCs. (**A**) Chemical structure of SN. (**B**) Effect of SN on the activity of NPCs. (**C**) Proliferation activity of NPCs in each experimental group. (**D**) ROS content in NPCs from each experimental group. (**E**) Initial wound size in the control group. (**F**) Initial wound size in the IL-1β treatment group. (**G**) Initial wound size in the SN+IL-1β treatment group. (**H**) Terminal wound size in the control group. (**I**) Terminal wound size in the IL-1β treatment group. (**J**) Terminal wound size in the SN+IL-1β treatment group. (**K**) Quantification of NPC's ability to heal wounds among different groups. (**L-O**) Apoptosis and quantification of NPCs were performed in each group, with data presented as mean ± standard deviation from three replicates per group. (**L**) is for control group. (**M**) is for IL-1β treatment group. (**N**) is for SN+IL-1β treatment group. **Indicates P < 0.01; ***indicates P < 0.001.

Abbreviation: SN, Sinomenine.

that seen in the IL-1β group (Figure 3A-H). qPCR and Western Blot analysis revealed that IL-1β significantly suppressed the expression of DCN and COL2A1, while promoting the expression of MMP3 and MMP13 in NPCs after 24 hours of treatment. However, this effect was effectively reversed by pre-treatment with SN for 8 hours (Figure 3I-Q).

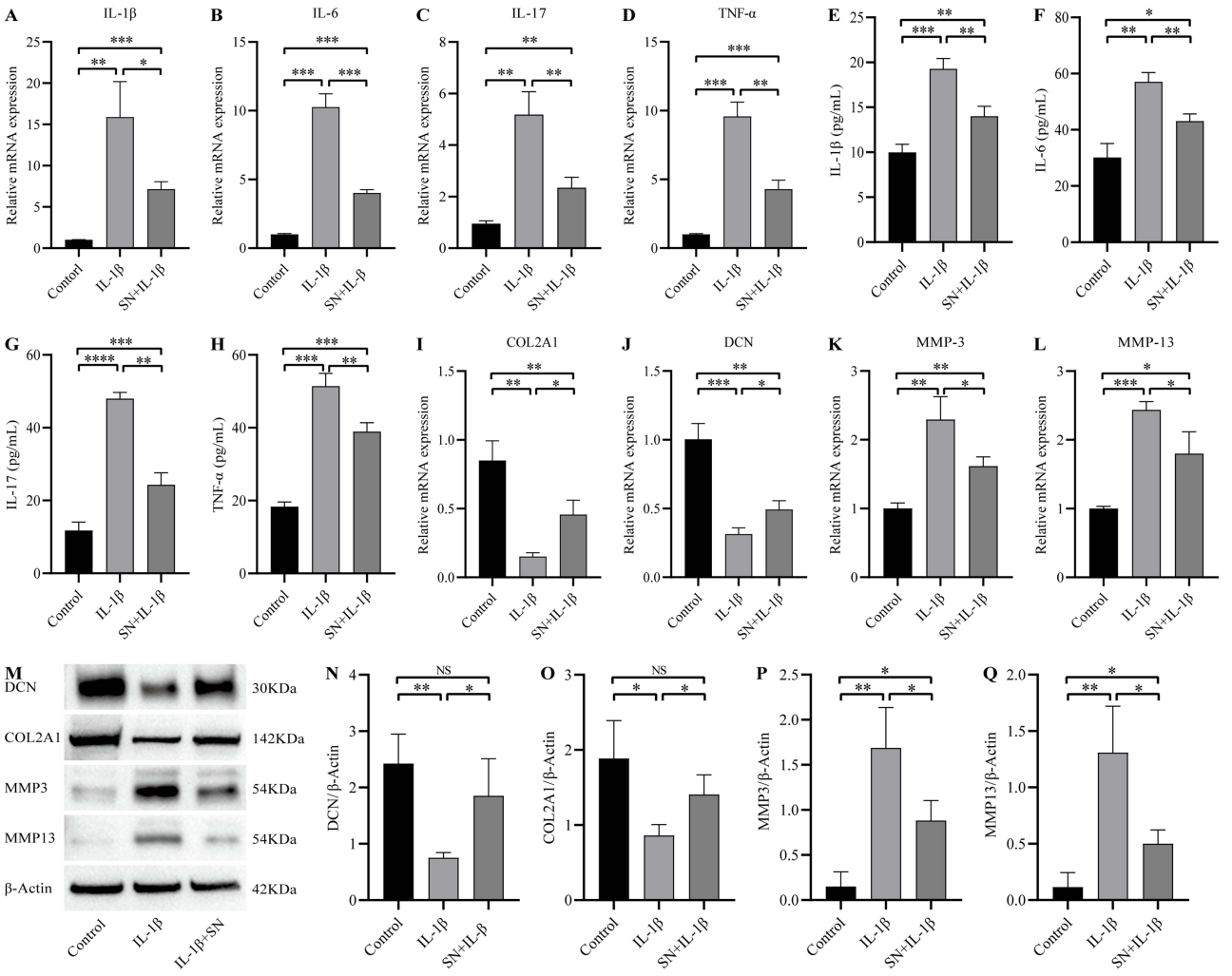

Figure 3 SN inhibited IL-1β-induced inflammation and improved cell phenotype in NPCs. (**A-D**) The transcription of mRNA for inflammatory factors (IL-1β, IL-6, IL-17, and TNF-α) was assessed in NPCs from each group. (**E-H**) ELISA was utilized to quantify the levels of inflammatory cytokines (IL-1β, IL-6, IL-17, TNF-α) in NPCs. (**I-L**) The transcription of mRNA for extracellular matrix-associated proteins was evaluated in NPCs from each group. (**M-Q**) Expression and quantification of extracellular matrix-related proteins were assessed in NPCs from each group, with β-actin serving as the reference. The data are presented as mean ± standard deviation. *indicates P <0.05, ** indicates P <0.01, *** indicates P <0.001, **** indicates P <0.0001, NS indicates that the difference was not statistically significant.

Abbreviations: SN, Sinomenine, DCN, Decorin, COL2A1, Alpha 1 type II collagen, MMP3, Matrix Metalloproteinase 3, MMP13, Matrix Metalloproteinase 13.

SN Suppressed IL-1β-Induced Apoptosis of NPCs by Modulating the Keap1/Nrf2 and NF-κB Signaling Pathways

To further elucidate the regulatory effect of SN on Keap1/Nrf2 and NF-κB signaling pathways, we pre-treated NPCs with Nrf2 inhibitor (Nrf2-in-1) or NF-κB agonist (SC) prior to subsequent treatment with IL-1β and/or SN. The results of the CCK-8 assay demonstrated that IL-1β significantly suppressed the proliferation activity of NPCs (P<0.001). However, pretreatment with SN significantly ameliorated this effect and improved the proliferation activity of NPCs (P<0.01). The proliferation activity of NPCs was inhibited when Nrf2 phosphorylation was suppressed by Nrf2-in-1 or NF-κB phosphorylation was promoted by SC (Figure 4A). Hoechst staining revealed an inverse correlation between the proliferation and apoptosis of NPCs. In the IL-1β group, pyknotic nuclei (apoptotic bodies) were observed, while the number of apoptotic bodies in the SN+IL-1β group was significantly lower than that in the IL-1β group (P<0.01). However, there was a significant increase in apoptotic bodies when Nrf2 phosphorylation was inhibited by Nrf2-in-1 or NF-κB phosphorylation was promoted by SC compared to the SN+IL-1β group (Figure 4B-G). qPCR analysis revealed that IL-1β significantly upregulated the mRNA expression of Keap1, Nrf2, HO-1, NQO-1 and NF-κB in NPCs from all groups. Furthermore, SN treatment further enhanced the mRNA levels of Keap1, Nrf2, HO-1 and NQO-1 while significantly reducing the content of NF-κB. Treatment with Nrf2-in-1 significantly reduced the mRNA levels of Keap1, Nrf2, HO-1, and NQO-1, while treatment with SC significantly increased the mRNA level of NF-κB (Figure 4H-L). The

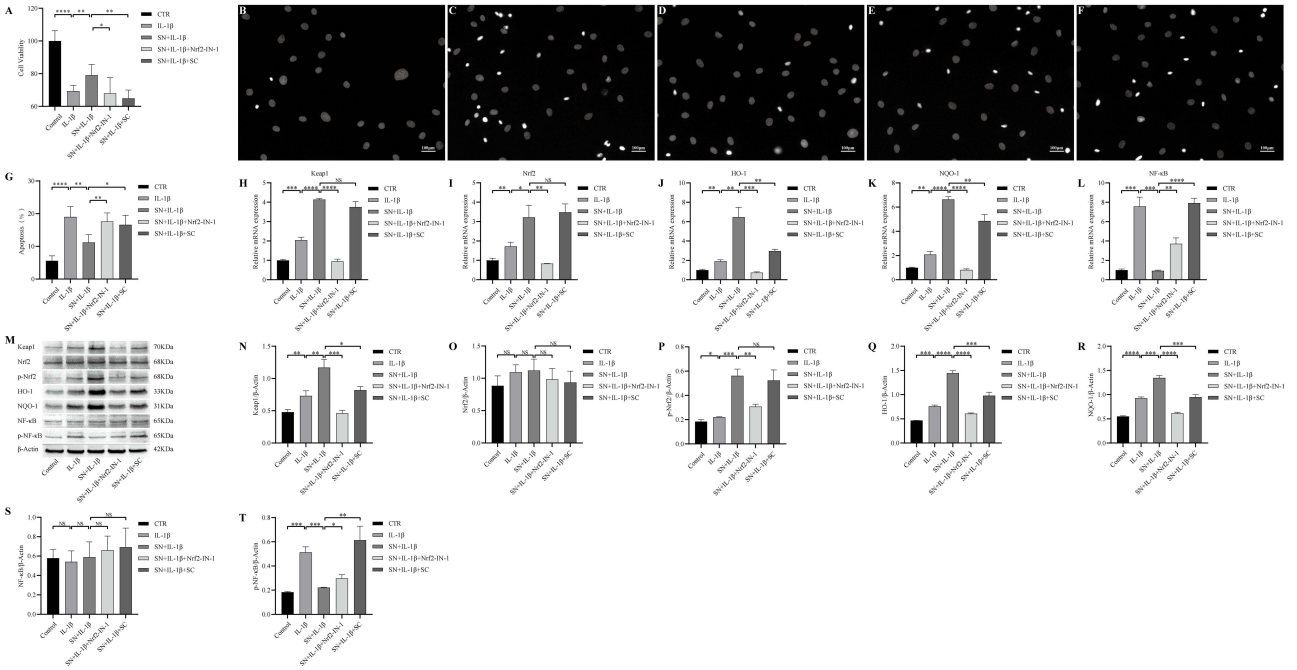

Figure 4 SN suppressed IL-1β-induced apoptosis of NPCs by modulating the Keap1/Nrf2 and NF-κB signaling pathways. (**A**) The CCK-8 assay was employed to determine the activity of NPCs in each group, with data presented as mean ± standard deviation and six replicates per group. (**B-G**) Apoptosis of NPCs in each group was assessed by Hoechst staining. The scale bar was 100μm in length. (**H-L**) mRNA transcription levels of Nrf2/HO-1 and NF-κB signaling pathway-related proteins were evaluated. (**M-T**) Expression and quantification analysis of Nrf2/HO-1 and NF-κB signaling pathway-related proteins were conducted, with β-actin serving as a reference. * indicates P <0.05, ** indicates P < 0.01, *** indicates P < 0.001, **** indicates P < 0.0001, NS, differences are not statistically significant.

Abbreviations: SN, Sinomenine; Nrf2-IN-1, Nrf2 inhibitor; SC, Sanguinarine Chloride (NF-κB activator); Keap1, Kelch-like ECH- associated protein 1; Nrf2, Nuclear factor erythroid 2-related factor 2; HO-1, Heme oxygenase-1; NQO-1, NAD(P)H quinone dehydrogenase 1; NF-κB, Nuclear factor kappa-light-chain-enhancer of activated B cells.

Western Blot results were consistent with those of qPCR, indicating that IL-1β significantly upregulated the expression of Keap1, p-Nrf2, HO-1, NQO-1 and p-NF-κB in NPCs across all groups. Furthermore, SN treatment further enhanced the expression of Keap1, p-Nrf2, HO-1 and NQO-1 while significantly reducing the expression of p-NF-κB. The treatment of Nrf2-IN-1 significantly reduced the expression of Keap1, p-Nrf2, HO-1 and NQO-1, while SC treatment significantly increased the expression of p-NF-κB. However, there was no significant change in the expression of Nrf2 and NF-κB among the groups (Figure 4M-T).

SN Improves IDD by Suppressing the Inflammatory Response

HE staining showed that the intervertebral space of the control IVD was highly normal, the fibrous rings were pink and neatly arranged in a ring-like stratification, the NPT was blue-purple and oval in shape, the volume was full, the extracellular matrix was abundant, and the inner Collagen II and Aggrecan were filled in the lattice-like chambers. The nuclei were stained blue and the cytoplasm was stained pink. The thickness of the upper and lower cartilage endplate (CEP) was high, and transparent chambers of varying sizes were visible within the CEP, which were filled with abundant collagen and cartilage endplate cells. After IL-1β treatment, the IVD intervertebral space height was reduced, the fibrous rings were broken and disorganized, and there was a large loss of nucleus pulposus tissue with residual white cavity. The thickness of the upper and lower CEP became thinner, and some of the CEP were destroyed, with no obvious cartilage component, and infiltrated by inflammatory cells. The above situation can be significantly improved with SN intervention (Figure 5A). Safranine O-fast green FCF cartilage stain showed good morphology of the IVD in the control group with normal intervertebral space height. The fibrous rings were neatly arranged in a ring-like stratification with green color. The nucleus pulposus was oval in shape, full in volume, rich in extracellular matrix, with Collagen II and Aggrecan filling the lattice-like chambers, red in proteoglycan, and blue-purple NPCs visible inside. After IL-1β treatment, the height of the IVD intervertebral space was reduced, the fibrous ring was broken and disorganized, and the nucleus pulposus was lost, leaving a white cavity. The thickness of the upper and lower CEP became thinner, and some CEP were destroyed without obvious cartilage components and infiltrated by inflammatory cells. These conditions can be significantly improved with SN intervention (Figure 5B). IVD pathology scores showed a significant increase with IL-1β treatment and a significant decrease with

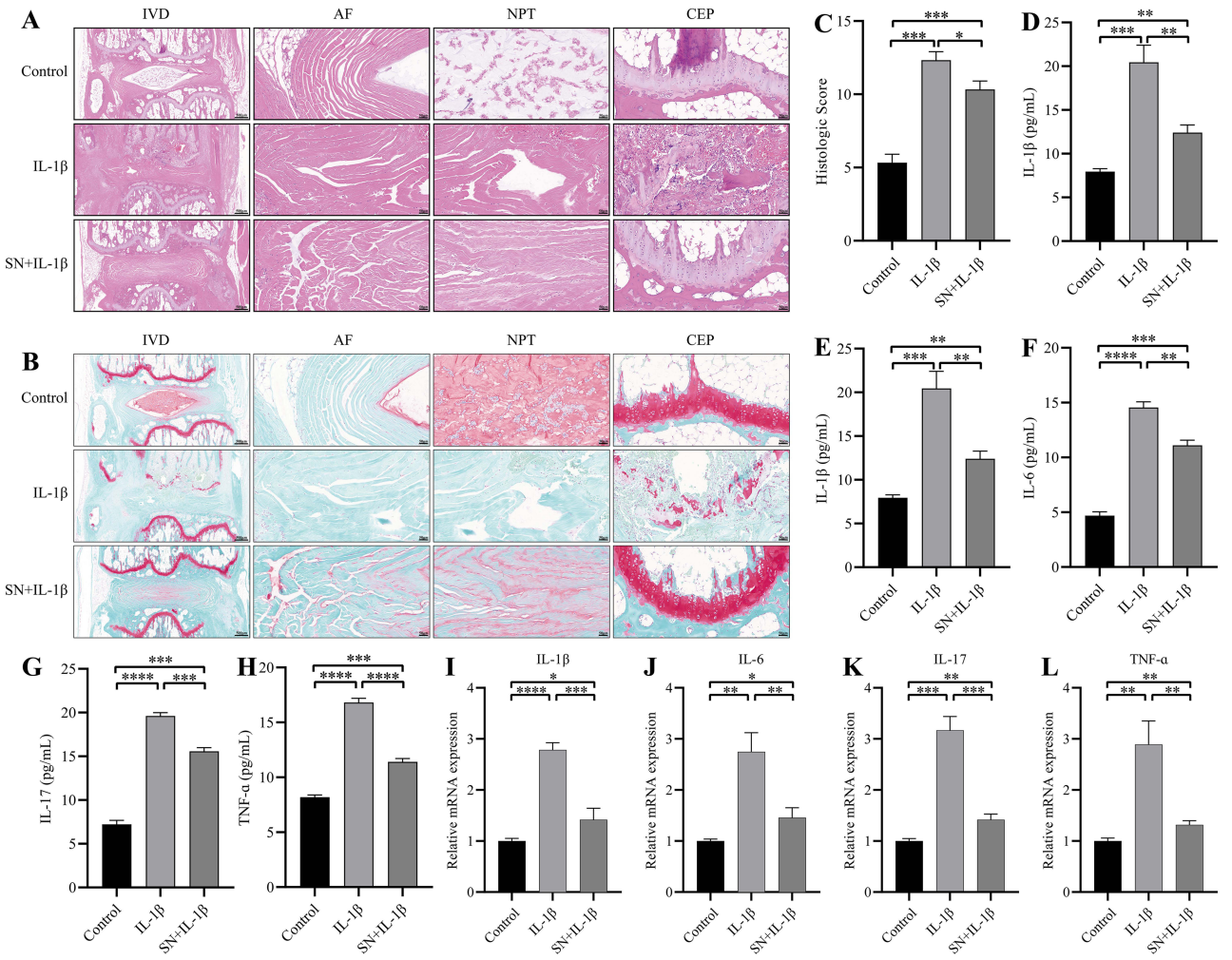

Figure 5 SN improves IDD by suppressing the inflammatory response. (**A**) IVD HE staining. (**B**) IVD staining with red O solid green is shown. The scale bar within the IVD column measures 500μm, while in the AF, NPT, and CEP columns it measures 50μm. (**C**) IVD pathology score. (**D-G**) ELisa assay of inflammatory factors (IL-1β, IL-6, IL-17, TNF-α) in each group of IVD. (**H-L**) mRNA transcripts of inflammatory factors (IL-1β, IL-6, IL-17, TNF-α) in each group of IVD profiles. Data are expressed as mean ± standard deviation, and β-actin was used as a reference. * indicates P <0.05, ** indicates P < 0.01; *** indicates P < 0.001; **** indicates P < 0.0001.
Abbreviations: SN, Sinomenine; IVD, Intervertebral Disc; AF, Annulus Fibrosus; NPT, Nucleus Pulposus Tissue; CEP, Cartilage Endplate.

SN intervention (Figure 5C). qPCR and ELisa assays showed a significant increase in the expression of inflammatory factors (IL-1β, IL-6, IL-17 and TNF-α) in IVD after IL-1β treatment, and when pretreated with SN, the inflammatory factor expression, although still significantly increased compared to the control group, was significantly reduced compared to the IL-1β group (Figure 5D-L).

SN Improves IDD by Regulating Keap1/Nrf2 and NF-κB Signaling Pathways

The qPCR and Western Blot assays showed that IL-1β treatment of IVD (IL-1β group) could, to some extent, promote the expression of Keap1, p-Nrf2, HO-1, NQO-1, significantly promote the expression of p-NF-κB, MMP3 and MMP13, and significantly inhibit the expression of DCN and COL2A1 compared with the control group. Treatment with SN significantly promoted the expression of Keap1, p-Nrf2, HO-1, NQO-1, DCN and COL2A1 and significantly inhibited the expression of p-NF-κB, MMP3 and MMP13 compared with the IL-1β group. There was no significant difference in Nrf2 and NF-κB protein expression in each group (Figure 6).

Discussion

In this study, we investigated the molecular mechanism underlying the inhibitory effect of SN on IDD. Our findings suggest that SN can suppress IL-1β-induced IDD by activating the Keap/Nrf2 signaling pathway, upregulating

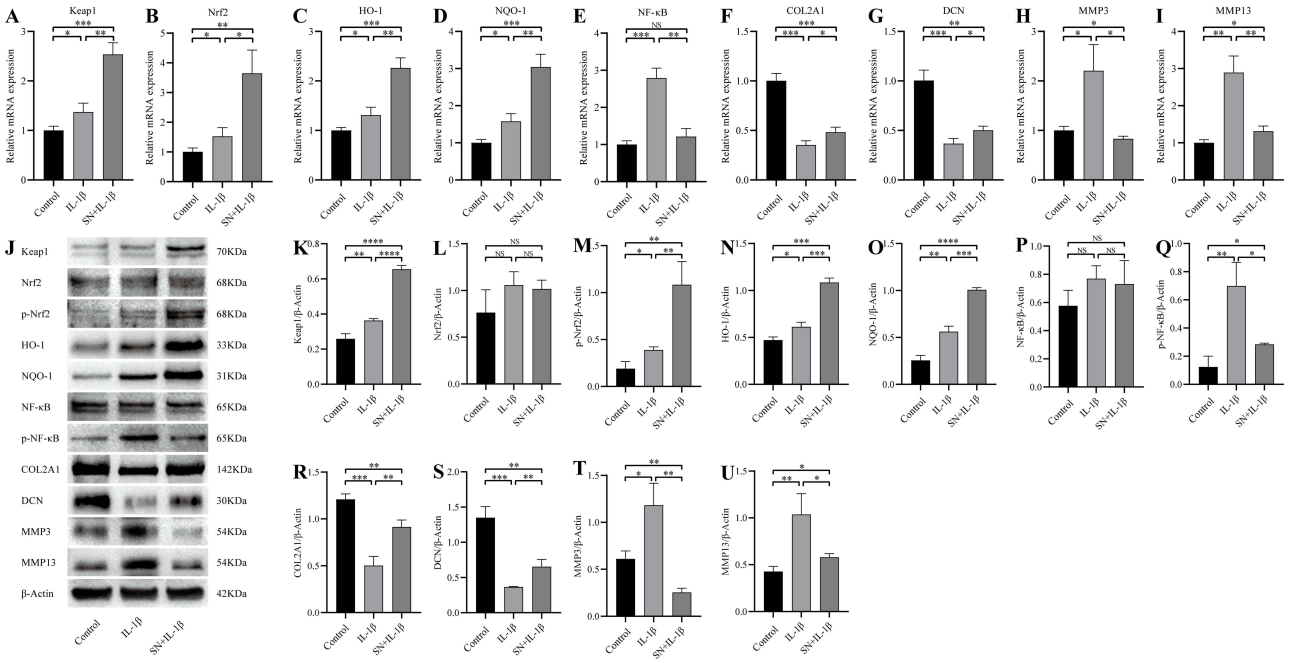

Figure 6 SN improves IDD by regulating Keap1/Nrf2 and NF-κB signaling pathways. (**A-I**) mRNA transcripts of Nrf2/HO-1 and NF-κB signaling pathways and extracellular matrix-associated proteins in each group of IVD. (**J-U**) Expression and quantification of Nrf2/HO-1 and NF-κB signaling pathways and extracellular matrix-associated proteins in each group of IVD. Data are expressed as mean ± standard deviation, and β-actin was used as reference. *Indicates P <0.05, ** indicates P < 0.01; *** indicates P < 0.001; ****Indicates P < 0.0001, NS, differences were not statistically significant.

Abbreviations: SN, Sinomenine; Keap1, Kelch-like ECH-associated protein 1; Nrf2, Nuclear factor erythroid 2-related factor 2; HO-1, Heme oxygenase-1; NQO-1, NAD(P)H quinone dehydrogenase 1; NF-κB, Nuclear factor kappa-light-chain-enhancer of activated B cells; COL2A1, Collagen Type II Alpha 1 Chain; DCN, Decorin; MMP3, Matrix Metalloproteinase 3; MMP13, Matrix Metalloproteinase 13.

antioxidant proteins such as HO-1 and NQO-1, reducing oxidative stress levels, and downregulating the NF-κB signaling pathway to attenuate inflammatory responses.

Oxidative stress and inflammatory factors have been identified as the primary pathogenic factors in the complex pathophysiological process and pathogenic mechanism of IDD.[14,15] Therefore, it is crucial to regulate the release of inflammatory factors and inhibit oxidative stress levels within the IVD for both prevention and treatment of IDD. To simulate the microenvironment of IDD characterized by inflammation and oxidative stress, we induced NPCs with IL-1β to establish an IDD model,[16,17] and intervened with SN to investigate its potential in inhibiting IDD. Our findings suggest that IL-1β not only triggers an inflammatory response in NPCs, resulting in a significant upregulation of IL-1β, IL-6, IL-17 and TNF-α synthesis, but also induces ROS accumulation, enhanced apoptosis, reduced proliferative activity and impaired wound healing capacity in NPCs. We observed a significant reduction in extracellular matrix proteins, such as DCN and COL2A1, synthesized by NPCs. Additionally, there was a notable increase in enzymes that degrade the extracellular matrix, including MMP3 and MMP13. These findings are consistent with the pathological changes seen in IDD and suggest that we have successfully replicated the inflammatory and oxidative microenvironment of IDD in vitro to construct an NPC-based model of this condition.

It is well-established that IL-1β can activate the NF-κB signaling pathway, thereby promoting the synthesis of downstream inflammatory factors.[18] Consequently, IL-1β is frequently employed as an inflammatory inducer to establish a pro-inflammatory milieu within cells and tissues. This also accounts for the marked increase in IL-1β, IL-6, IL-17 and TNF-α synthesis observed following treatment with this cytokine in NPCs. What is the mechanism underlying IL-1β-induced ROS accumulation in NPCs and how does this relate to the synthesis of inflammatory mediators? Hu et al demonstrated that IL-1β triggers necroptosis and NLRP3 inflammasome activation in NPCs, accompanied by mitochondrial oxidative stress damage and dysfunction.[19] Similarly, Zhang et al reported that IL-1β induces oxidative stress injury in NPCs,[20] yet the underlying mechanisms of ROS accumulation remain elusive. We propose that IL-1β triggers the mitochondrial apoptotic pathway in NPCs, resulting in a reduction of the Bcl-2/Bax ratio, damage to the mitochondrial

membrane, and release of cytochrome C into the cytoplasm where it binds with Apaf-1 to form an apoptotic complex. This complex recruits and cleaves caspase-9 precursors leading to their activation. Activated Caspase-9 can further activate Caspase-3 which ultimately leads to apoptosis of NPCs. As a consequence of damage to the mitochondrial membrane, electron transfer is impeded, resulting in incomplete utilization of oxygen for reduction to water molecules and generation of superoxide ions (ROS). When ROS production surpasses the capacity of intracellular redox system, it leads to ROS accumulation.[21] Therefore, the IL-1β-induced apoptosis of NPCs leading to IDD is closely associated with the IL-1β-triggered inflammatory response and oxidative stress damage. To investigate the mechanism underlying IL-1β-induced IDD and evaluate the therapeutic potential of SN, we pre-treated NPCs with SN prior to exposure to IL-1β, thereby establishing an IDD model. Our findings demonstrate that all IDD-related parameters were significantly ameliorated by SN treatment, which may be attributed to its anti-inflammatory and antioxidant properties; however, further investigation is warranted to elucidate the precise mechanisms involved.

The Keap/Nrf2 signaling pathway is a crucial intracellular player in oxidative stress and plays a pivotal role in regulating the intracellular response to oxidative stress. Under physiological conditions, Nrf2 is subjected to ubiquitination upon binding with Keap1. The resulting ubiquitinated Nrf2 can be degraded by the 26S proteasome, thereby maintaining a low intracellular level of Nrf2. When cells experience oxidative stress damage, Keap1's ability to ubiquitinate Nrf2 is compromised. This results in the transfer of Nrf2 phosphorylation from the cytoplasm to the nucleus, where it binds with target gene ARE/EpRE and triggers the expression of a range of antioxidant enzymes such as HO-1 and NQO-1.[22,23] The NF-κB signaling pathway plays a pivotal role in the regulation of inflammation and immune response. Under physiological conditions, NF-κB proteins typically form homo/heterodimers from p65 and p50 subunits, which are sequestered in the cytoplasm by binding to inhibitory protein IkB to form a trimeric complex. When IL-1β, the upstream signaling factor, binds to the cell membrane surface receptor, it induces a conformational change in the receptor that transmits the signal to IKK kinase (IkB kinase), resulting in phosphorylation of IkB protein and subsequent dissociation from the trimer. Subsequently, NF-κB dimers expose nuclear localization sequences (NLS) and rapidly translocate from the cytoplasm to the nucleus to bind specific sequences on nuclear DNA, thereby promoting transcription of related genes such as CyclinD1, c-Myc, MMP-9, VEGF etc. Therefore, modulation of Keap/Nrf2 and NF-κB signaling pathways can effectively ameliorate intracellular oxidative stress and inflammation.

Studies have demonstrated the effective regulation of Keap/Nrf2 and NF-κB signaling pathways by SN. In a mouse model of OA, Yu et al observed that SN exerts therapeutic effects on OA by inhibiting the release of inflammatory factors and degradation of extracellular matrix through activation of Nrf2/HO-1 signaling pathway and inhibition of NF-κB signaling pathway.[24] Cao et al demonstrated that SN exerts anti-inflammatory and nephroprotective effects by modulating the Keap1/Nrf2 and NF-κB signaling pathways in a mouse model of nephropathy.[25] Therefore, we postulate that SN may similarly attenuate IDD via regulation of the Keap1/Nrf2 and NF-κB signaling pathways in NPCs. To test our conjecture, we used an Nrf2 inhibitor (Nrf2-IN-1) and an NF-κB agonist (SC) to interfere with the activity of the Keap1/Nrf2 and NF-κB signaling pathways. The findings demonstrated that SN significantly activated the Keap1/Nrf2 signaling pathway, thereby promoting the expression of downstream antioxidant proteins such as HO-1 and NQO-1. Additionally, it inhibited the activation of NF-κB signaling pathway and ameliorated IL-1β-induced decrease in proliferative activity and increase in apoptosis of myeloid cells. The cytoprotective effect of SN was significantly attenuated upon inhibition of Keap1/Nrf2 signaling activation or promotion of NF-κB signaling pathway activation. The aforementioned results strongly support our argument. However, we did not further investigate the role relationship between the Keap1/Nrf2 signaling pathway and the NF-κB signaling pathway. According to literature, HO-1's metabolic end products have been shown to inhibit NF-κB translocation into the nucleus, thereby suppressing downstream gene expression.[26,27] Furthermore, the activity of NF-κB is regulated by various post-translational phosphorylation modifications, with the phosphorylation of RelA/p65 at Ser276 particularly influenced by ROS. ROS can modify cellular molecules, including DNA. One prevalent oxidation product is 8-oxo-7,8-dihydroguanine (8-oxoGua), which can be repaired through the base excision repair pathway initiated by 8-oxoguanine DNA glycosylase 1 (OGG1). Recently, OGG1 has been found to have a novel function in binding to 8-oxoGua and enhancing transcription of pro-inflammatory cytokines and chemokines. Wang et al demonstrated that the interaction between DNA-bound OGG1 and mitogen-and stress-activated kinase 1 (MSK1) plays a crucial role in RelA/p65 Ser276 phosphorylation. Scavenging ROS or depleting/inhibiting OGG1

hindered the MSK1 and RelA/p65 interaction, resulting in reduced phospho-Ser276 levels and significantly decreased expression of ROS-responsive cytokine/chemokine genes.[28] This may be a key mechanism by which the Keap1/Nrf2 signaling pathway links the NF-κB signaling pathway.

The extracellular matrix (ECM) provides a favorable microenvironment for the survival of NPCs and plays a crucial role in maintaining IVD function.[29] NPCs are primarily responsible for synthesizing and secreting ECM, which mainly consists of type II collagen and core proteoglycans. Studies have demonstrated that degenerated IVD tissue exhibits a significant reduction in ECM content, while the levels of ECM-degrading enzymes such as MMP3, MMP13, ADAMTS4, and ADAMTS5 are significantly elevated.[30] Therefore, repression of ECM-degrading enzymes and promotion of ECM synthesis are crucial for the prevention and management of IDD. To further investigate the role of SN in a rat model of IDD, we established an IDD model by combining acupuncture and IL-1β injection, followed by intervention with SN. The results indicated significant degeneration of the IVD in the model group, characterized by fibrous ring rupture and disorganization, loss of intervertebral height, cartilage endplate damage, and nucleus pulposus tissue loss. Additionally, there was notable activation of the NF-κB signaling pathway along with marked increases in inflammatory factors MMP3 and MMP13 while Collagen II and DCN levels decreased significantly. When SN intervention was applied, the Keap1/Nrf2 signaling pathway was significantly activated, while the NF-κB signaling pathway was significantly inhibited, leading to significant improvements in IDD outcomes. These findings are consistent with those of Gao and Liu et al, except that they investigated the mechanism of SN inhibition of IDD from the perspective of SN regulation of autophagy and macrophage polarization in NPCs.[13,31]

Conclusion

In summary, our study demonstrates that SN plays a crucial role in mitigating the development of IDD by activating the Keap1/Nrf2 signaling pathway and inhibiting the NF-κB signaling pathway. These findings provide novel insights into understanding and treating IDD.

Acknowledgments

The authors thank Shulong Jiang and Luning Li (Clinical Medicine Laboratory Center, Jining No.1 People's Hospital, Jining Medical University, Jining, China) for technical assistance.

Author Contributions

All authors made a significant contribution to the work reported, whether that is in the conception, study design, execution, acquisition of data, analysis and interpretation, or in all these areas; took part in drafting, revising or critically reviewing the article; gave final approval of the version to be published; have agreed on the journal to which the article has been submitted; and agree to be accountable for all aspects of the work.

Funding

This research was funded by Natural Science Foundation of Shandong Province, grant number ZR2021LZY008; Shandong Traditional Chinese Medicine Science and Technology Project, grant number Q-2022025; Jining City Key Research and Development Program Project, grant number 2020JKNS008 and Shandong Province Medical and Health Science and Technology Development Plan Project, grant number 202104070383.

Disclosure

The authors report no conflicts of interest in this work.

References

1. Barr JS, Riseborough EJ. Treatment of low back and sciatic pain in patients over 60 years of age. A study of 100 patients. *Clin Orthop Relat Res*. 1963;26:12–18.
2. Mixter WJ. RUPTURE OF THE LUMBAR INTERVERTEBRAL DISK: AN ETIOLOGIC FACTOR FOR SO-CALLED "SCIATIC" PAIN. *Ann Surg*. 1937;106(4):777–787. doi:10.1097/00000658-193710000-00027

3. Denes K, Aranyi Z, Csillik A, et al. [Serum biomarkers in acute low back pain and sciatica].. *Orv Hetil*. 2020;161(13):483–490. doi:10.1556/650.2020.31665
4. Jungen MJ, Ter Meulen BC, van Osch T, Weinstein HC, Ostelo R. Inflammatory biomarkers in patients with sciatica: a systematic review. *BMC Musculoskelet Disord*. 2019;20(1):156. doi:10.1186/s12891-019-2541-0
5. Wang Y, Che M, Xin J, et al. The role of IL-1beta and TNF-alpha in intervertebral disc degeneration. *Biomed Pharmacother*. 2020;131:110660. doi:10.1016/j.biopha.2020.110660
6. Zhao K, An R, Xiang Q, et al. Acid-sensing ion channels regulate nucleus pulposus cell inflammation and pyroptosis via the NLRP3 inflammasome in intervertebral disc degeneration. *Cell Prolif*. 2021;54(1):e12941. doi:10.1111/cpr.12941
7. Xu Q, Xing H, Wu J, Chen W, Zhang N. miRNA-141 Induced Pyroptosis in Intervertebral Disk Degeneration by Targeting ROS Generation and Activating TXNIP/NLRP3 Signaling in Nucleus Pulposus Cells. *Front Cell Dev Biol*. 2020;8:871. doi:10.3389/fcell.2020.00871
8. Jiang W, Fan W, Gao T, et al. Analgesic Mechanism of Sinomenine against Chronic Pain. *Pain Res Manag*. 2020;2020:1876862. doi:10.1155/2020/1876862
9. Zhang YS, Han JY, Iqbal O, Liang AH. Research Advances and Prospects on Mechanism of Sinomenin on Histamine Release and the Binding to Histamine Receptors. *Int J Mol Sci*. 2018;20(1):70. doi:10.3390/ijms20010070
10. Fan H, Shu Q, Guan X, et al. Sinomenine Protects PC12 Neuronal Cells against H(2)O(2)-induced Cytotoxicity and Oxidative Stress via a ROS-dependent Up-regulation of Endogenous Antioxidant System. *Cell Mol Neurobiol*. 2017;37(8):1387–1398. doi:10.1007/s10571-017-0469-1
11. Liu W, Zhang Y, Zhu W, et al. Sinomenine Inhibits the Progression of Rheumatoid Arthritis by Regulating the Secretion of Inflammatory Cytokines and Monocyte/Macrophage Subsets. *Front Immunol*. 2018;9:2228. doi:10.3389/fimmu.2018.02228
12. Zeng MY, Tong QY. Anti-inflammation Effects of Sinomenine on Macrophages through Suppressing Activated TLR4/NF-kappaB Signaling Pathway. *Curr Med Sci*. 2020;40(1):130–137. doi:10.1007/s11596-020-2156-6
13. Gao Z, Lin Y, Zhang P, et al. Sinomenine ameliorates intervertebral disc degeneration via inhibition of apoptosis and autophagy in vitro and in vivo. *Am J Transl Res*. 2019;11(9):5956–5966.
14. Wang Y, Cheng H, Wang T, et al. Oxidative stress in intervertebral disc degeneration: molecular mechanisms, pathogenesis and treatment. *Cell Prolif*. 2023;56(9):e13448. doi:10.1111/cpr.13448
15. Shnayder NA, Ashkhotov AV, Trefilova VV, et al. Molecular Basic of Pharmacotherapy of Cytokine Imbalance as a Component of Intervertebral Disc Degeneration Treatment. *Int J Mol Sci*. 2023;24(9):56.
16. Wang K, Yao D, Li Y, et al. TAK-715 alleviated IL-1beta-induced apoptosis and ECM degradation in nucleus pulposus cells and attenuated intervertebral disc degeneration ex vivo and in vivo. *Arthritis Res Ther*. 2023;25(1):45. doi:10.1186/s13075-023-03028-4
17. Zhu F, Duan W, Zhong C, Ji B, Liu X. The protective effects of dezocine on interleukin-1beta-induced inflammation, oxidative stress and apoptosis of human nucleus pulposus cells and the possible mechanisms. *Bioengineered*. 2022;13(1):1399–1410. doi:10.1080/21655979.2021.2017700
18. Zhu X, Guo S, Zhang M, Bai X. Emodin protects against apoptosis and inflammation by regulating reactive oxygen species-mediated NF-kappaB signaling in interleukin-1beta-stimulated human nucleus pulposus cells. *Hum Exp Toxicol*. 2023;42:9603271221138552. doi:10.1177/09603271221138552
19. Ma Z, Tang P, Dong W, et al. SIRT1 alleviates IL-1beta induced nucleus pulposus cells pyroptosis via mitophagy in intervertebral disc degeneration. *Int Immunopharmacol*. 2022;107:108671. doi:10.1016/j.intimp.2022.108671
20. Bai X, Yao M, Zhu X, Lian Y, Zhang M. Baicalin suppresses interleukin-1beta-induced apoptosis, inflammatory response, oxidative stress, and extracellular matrix degradation in human nucleus pulposus cells. *Immunopharmacol Immunotoxicol*. 2023;1–10.
21. Shen J, Xu S, Zhou H, et al. IL-1beta induces apoptosis and autophagy via mitochondria pathway in human degenerative nucleus pulposus cells. *Sci Rep*. 2017;7(1):41067. doi:10.1038/srep41067
22. Yamamoto M, Kensler TW, Motohashi H. The KEAP1-NRF2 System: a Thiol-Based Sensor-Effector Apparatus for Maintaining Redox Homeostasis. *Physiol Rev*. 2018;98(3):1169–1203. doi:10.1152/physrev.00023.2017
23. Dayalan NS, Dinkova-Kostova AT. KEAP1, a cysteine-based sensor and a drug target for the prevention and treatment of chronic disease. *Open Biol*. 2020;10(6):200105. doi:10.1098/rsob.200105
24. Wu Y, Lin Z, Yan Z, et al. Sinomenine contributes to the inhibition of the inflammatory response and the improvement of osteoarthritis in mouse-cartilage cells by acting on the Nrf2/HO-1 and NF-kappaB signaling pathways. *Int Immunopharmacol*. 2019;75:105715. doi:10.1016/j.intimp.2019.105715
25. Qin T, Du R, Huang F, et al. Sinomenine activation of Nrf2 signaling prevents hyperactive inflammation and kidney injury in a mouse model of obstructive nephropathy. *Free Radic Biol Med*. 2016;92:90–99. doi:10.1016/j.freeradbiomed.2016.01.011
26. Bellezza I, Tucci A, Galli F, et al. Inhibition of NF-kappaB nuclear translocation via HO-1 activation underlies alpha-tocopheryl succinate toxicity. *J Nutr Biochem*. 2012;23(12):1583–1591. doi:10.1016/j.jnutbio.2011.10.012
27. Zhang P, Jin Y, Xia W, Wang X, Zhou Z. Phillygenin inhibits inflammation in chondrocytes via the Nrf2/NF-kappaB axis and ameliorates osteoarthritis in mice. *J Orthop Translat*. 2023;41:1–11. doi:10.1016/j.jot.2023.03.002
28. Xue Y, Li C, Deng S, et al. 8-Oxoguanine DNA glycosylase 1 selectively modulates ROS-responsive NF-κB targets through recruitment of MSK1 and phosphorylation of RelA/p65 at Ser276. *J Biol Chem*. 2023;29:105308. doi:10.1016/j.jbc.2023.105308
29. Peng Y, Chen X, Liu S, et al. Extracellular Vesicle-Conjugated Functional Matrix Hydrogels Prevent Senescence by Exosomal miR-3594-5p-Targeted HIPK2/p53 Pathway for Disc Regeneration. *Small*. 2023;19(37):e2206888. doi:10.1002/smll.202206888
30. Yu X, Liu Q, Wang Y, et al. Depleted Long Noncoding RNA GAS5 Relieves Intervertebral Disc Degeneration via microRNA-17-3p/Ang-2. *Oxid Med Cell Longev*. 2022;2022:1792412. doi:10.1155/2022/1792412
31. Hou X, Shen Y, Sun M, et al. Effect of regulating macrophage polarization phenotype on intervertebral disc degeneration. *Immun Inflamm Dis*. 2022;10(11):e714. doi:10.1002/iid3.714